Inorg. Chem. **2006**, *45*, 591–598

Supramolecular Assembly of Gold(I) Complexes of Diphosphines and *N,N′*-Bis-4-methylpyridyl Oxalamide

Biing-Chiau Tzeng,*,† Hsien-Te Yeh,† Ya-Ling Wu,† Jau-Huei Kuo,† Gene-Hsiang Lee,‡ and Shie-Ming Peng‡

Department of Chemistry and Biochemistry, National Chung Cheng University, 168, University Road, Min-Hsiung, Chia-Yi, Taiwan 621, and Department of Chemistry, National Taiwan University, 1, Sec. 4, Roosevelt Road, Taipei, Taiwan 106

Received August 1, 2005

We report herein the supramolecular assembly and spectroscopic and luminescent properties of gold(I) complexes of diphosphines (dppm [bis(diphenylphosphino)methane], dppp [1,3-bis(diphenylphosphino)propane], and dpppn [1,5-bis(diphenylphosphino)pentane]) and *N,N′*-bis-4-methylpyridyl oxalamide (**L**). The dppm and dppp cases form the rectangular structures, $[dppm(Au_2)\mathbf{L}]_2(ClO_4)_4$ and $[dppp(Au_2)\mathbf{L}]_2(ClO_4)_4$, with four gold(I) ions at the corners, as well as two **L** and two dppm or dppp ligands as edges, featuring 38- and 42-membered rings for the former and the latter, respectively. Remarkably, the packing of the dppp complexes shows interesting one-dimensional rectangular channels in the solid state, most likely due to intermolecular $\pi\cdots\pi$ interactions. The dpppn complex has been structurally characterized as a one-dimensional coordination polymer, $\{[(dpppn)_{3.5}(Au_7)\mathbf{L}_{3.5}](PF_6)_7\}$. The absorptions and emissions of the compounds are in general due to intraligand transitions, but aurophilic or $\pi\cdots\pi$ interactions could also make partial contributions. The dipyridyl amide system with the amides incorporated into the bridging ligands as well as the one-dimensional rectangular channels in the solid state for the dppp-based rectangle make this a promising family of metal-containing cyclic peptides in crystal engineering and molecular-recognition studies.

Introduction

The widespread use of the coordinative-bond approach in the construction of supramolecular coordination compounds by self-assembly is well established.[1] So far, a wide range of one-, two-, and three-dimensional infinite solid-state coordination architectures[2] as well as discrete supramolecular structures (i.e., triangles, squares, rectangles, etc.)[1] have been isolated and structurally characterized. A paradigm example of a supramolecular system, $[(en)Pd(4,4'\text{-bpy})]_4(NO_3)_8$ (en = ethylenediamine, 4,4′-bpy = 4,4′-bipyridyl), was first reported by Fujita et al.,[3a] and its molecular structure was determined by X-ray diffraction to be a molecular square,[3b] which is the most common structure for cyclic molecules based on multimetallic coordination chemistry achieving cavity alignment and channel formation in the solid state. Remarkably, $[Re(CO)_3X(diimine)]_4$ (X = Cl, Br; diimine = pyrazine, 4,4-bipyridine, or other linear spacers) complexes represent another interesting family of neutral molecular squares with tunable cavity sizes depending on the linear spacers used.[4] Moreover, Hupp et al have also obtained Mn-

* To whom correspondence should be addressed. E-mail: chebct@ccu.edu.tw.

† National Chung Cheng University.

‡ National Taiwan University.

(1) (a) Fujita, M. *Chem. Soc. Rev.* **1998**, *27*, 417. (b) Leininger, S.; Olenyuk, B.; Stang, P. J. *Chem. Rev.* **2000**, *100*, 853. (c) Holliday, B. A.; Mirkin, C. A. *Angew. Chem., Int. Ed.* **2001**, *40*, 2022. (d) Yaghi, O. M.; Li, H. L.; Davis, C.; Richardson, D.; Groy, T. L. *Acc. Chem. Res.* **1998**, *31*, 474. (e) Dinolfom, P. H.; Hupp, J. T. *Chem. Mater.* **2001**, *13*, 3113.

(2) (a) Li, H.; Eddaoudi, M.; O'Keeffe, M.; Yaghi, M. *Nature* **1999**, *402*, 276−279. (b) Swiegers, G. F.; Malefetse, T. J. *Chem. Rev.* **2000**, *100*, 3483−3537. (c) Zaworotko, M. J. *Nature* **1999**, *402*, 242−243. (d) Zaworotko, M. J. *Angew. Chem., Int. Ed.* **2000**, *39*, 3052−3054. (e) Batten, S. R.; Robson, R. *Angew. Chem., Int. Ed.* **1998**, *37*, 1461−1494. (f) Hagrman, P. J.; Hagrman, D.; Zubieta, J. *Angew. Chem., Int. Ed.* **1999**, *38*, 2639−2684.

(3) (a) Fujita, M.; Yazaki, J.; Ogura, K. *J. Am. Chem. Soc.* **1990**, *112*, 5645. (b) Fujita, M.; Sasaki, O.; Mitsuhashi, T.; Fujita, T.; Yazaki, J.; Yamaguchi, K.; Ogura, K. *Chem. Commun.* **1996**, 1535.

(4) (a) Slone, R. V.; Yoon, D. I.; Calhoun, R. M.; Hupp, J. T. *J. Am. Chem. Soc.* **1995**, *117*, 11813. (b) Slone, R. V.; Hupp, J. T.; Stern, C. L.; Albrecht-Schmitt, T. E. *Inorg. Chem.* **1996**, *35*, 4096. (c) Slone, R. V.; Hupp, J. T. *Inorg. Chem.* **1997**, *36*, 5422−5423. (d) Slone, R. V.; Benkstein, K. D.; Bélanger, S.; Hupp, J. T.; Guzei, I. A.; Rheingold, A, L. *Coord. Chem. Rev.* **1998**, *171*, 221. (e) Bélanger, S.; Keefe, M. H.; Welch, J.; Hupp, J. T. *Coord. Chem. Rev.* **1999**, *192*, 29.

10.1021/ic051297a CCC: $33.50
Published on Web 12/14/2005

(I) and Re(I) rectangles via a two-step synthesis,[5] where they found that chelating ligands were necessary for the formation of stable rectangles. Their attempts to obtain rectangular structures instead by using mixtures of short and long nonchelating ligands (spacers) such as pyrazine and 4,4′-bipyridine invariably failed, with quantitative disproportionation into small and large molecular squares. In addition, a handful examples of Re(I)-based rectangles were also reported by Lu and co-workers by a two-step synthesis or one-pot preparation.[6] Applications including chemical sieving, chemical sensing, and catalysis based on squares, rectangles, and related supermolecules have been found, and some complexes have shown exciting effects.[7] While molecular squares have been synthesized, there are relatively few molecular rectangles.

The propensity for closed-shell d^{10} gold(I) centers to have weak bonding interactions, leading to a variety of supramolecular gold(I) compounds with novel structural and intriguing spectroscopic properties, has been an interesting aspect of gold chemistry.[8,9] These interactions are typically identified by means of X-ray diffraction studies, where gold(I)···gold(I) distances are less than or close to the sum of the van der Waals radii (3.32 Å).[10] The presence of aurophilic contacts may be recognized not only by short gold(I)···gold(I) distances and novel structural features, but also by intriguing electronic absorption and luminescent properties. Puddephatt et al. have recently further demonstrated the application of aurophilicity in the construction of supramolecular gold(I)-containing rings and catenanes by a self-assembly process.[11] The potential for two-coordinate geometry as well as the tendency for gold(I) ions to aggregate in the solid state are expected to contribute to the formation of novel supramolecular structures. Thus, the pioneering work of Puddephatt has opened the door to the construction of a novel family of gold(I)-containing supermolecules.

Amides have proven to be very useful in self-assembly processes through hydrogen bonding, and the assembled products are relevant to biological systems. Remarkably, Ghadiri et al. first published their delicate work in 1994 regarding the formation of nanotube frameworks with a diameter of 1.3 nm built from polypeptide bonds as basic subunits as well as through inter-ring NH···O═C hydrogen bonds.[12] These nanotubes represent a new and important class of functional materials. In this context, we initiated the study of metal-containing cyclic amides, featuring cyclic peptides. Recently, there has been much interest in molecular loops, triangles, or squares, assembled through coordination chemistry. However, the stacking has usually been unpredictable, and so the discovery of stacked supermolecules in these systems has often been serendipitous. This is particularly important to search for the driving force in supramolecular systems to direct the macrocyclic molecules to stack into the well-ordered one-dimensional channel structures in the solid state and/or thin films. By taking advantage of the uniform channel structures, the selective VOC (volatile organic compounds) sensing and size-selective transport properties by molecular thin-film materials reported by Hupp et al. may prove useful in subsequent catalytic, ultrafiltration, and chemical sensing applications.[4] The biomimetic approach to organization of molecular loops and other macrocyclic structures has considerable promise. In addition, the amide−amide hydrogen bonding has been shown to increase the supramolecular complexity[13] and may function as a receptor site for recognition events. We report herein the supramolecular assembly and spectroscopic and luminescent properties of gold(I) compounds with diphosphines (i.e., dppm [bis(diphenylphosphino)methane], dppp [1,3-bis(diphenylphosphino)propane], and dpppn [1,5-bis(diphenylphosphino)-pentane]) and *N*,*N*′-bis-4-methylpyridyl oxalamide (**L**).

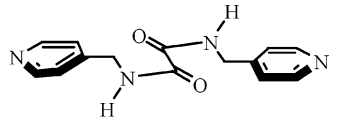

L

(5) (a) Benkstein, K. D.; Hupp, J. T.; Stern, C. L. *Inorg. Chem.* **1998**, *37*, 5404. (b) Benkstein, K. D.; Hupp, J. T.; Stern, C. L. *J. Am. Chem. Soc.* **1998**, *120*, 12982. (c) Benkstein, K. D.; Hupp, J. T.; Stern, C. L. *Angew. Chem., Int. Ed.* **2000**, *39*, 2891.

(6) (a) Rajendran, T.; Manimaran, B.; Lee, F.-Y.; Lee, G.-H.; Peng, S.-M.; Wang, C.-M.; Lu, K.-L. *Inorg. Chem.* **2000**, *39*, 2016. (b) Manimaran, B.; Rajendran, T.; Lu, Y.-L.; Lee, G.-H.; Peng, S.-M.; Lu, K.-L. *J. Chem. Soc., Dalton Trans.* **2001**, 515. (c) Manimaran, B.; Thanasekaran, P.; Rajendran, T.; Lin, R.-J.; Chang, I.-J.; Lee, G.-H.; Peng, S.-M.; Rajagopal, S.; Lu, K.-L. *Inorg. Chem.* **2002**, *41*, 21. (d) Rajendran, T.; Manimaran, B.; Liao, R.-T.; Lin, R.-J.; Thanasekaran, P.; Lee, G.-H.; Peng, S.-M.; Liu, Y.-H.; Chang, I.-J.; Rajagopal, S.; Lu, K.-L. *Inorg. Chem.* **2003**, *42*, 6388. (e) Thanasekaran, P.; Liao, R.-T.; Liu, Y.-H.; Rajendran, T.; Rajagopal, S.; Lu, K.-L. *Coord. Chem. Rev.* **2005**, *249*, 1085.

(7) (a) Bélanger, S.; Hupp, J. T.; Stern, C. L.; Slone, R. V.; Watson, D. F.; Carrell, T. M. *J. Am. Chem.* Soc. **1999**, *121*, 557. (b) Bélanger, S.; Hupp, J. T. *Angew. Chem., Int. Ed.* **1999**, *38*, 2222. (c) Mines, G. A.; Tzeng, B.-C.; Stevenson, K. J.; Li, J.; Hupp, J. T. *Angew. Chem., Int. Ed.* **2002**, *41*, 154. (d) Keefe, M. H.; Slone, R. V.; Hupp, J. T.; Czaplewski, K. F.; Snurr, R. Q.; Stern, C. L. *Langmuir* **2000**, *16*, 3964. (e) Merlau, M. L.; Mejia, M. d. P.; Nguyen, S. T.; Hupp, J. T. *Angew. Chem., Int. Ed.* **2001**, *40*, 4239. (f) Sun, S. S.; Lees, A. J. *J. Am. Chem. Soc.* **2000**, *122*, 8956. (g) Tashiro, S.; Tominaga, M.; Kawano, M.; Therrien, B.; Ozeki, T.; Fujita, M. *J. Am. Chem. Soc.* **2005**, *127*, 4546. (h) Yoshizawa, M.; Takeyama, Y.; Okano, T.; Fujita, M. *J. Am. Chem.* Soc. **2003**, *125*, 3243.

(8) (a) Pyykkö, P. *Chem. Rev.* **1997**, *97*, 597. (b) Pyykkö, P.; Zhao, Y. *Angew. Chem., Int. Ed. Engl.* **1995**, *34*, 1894. (c) Pyykkö, P.; Li, J.; Runeberg, N. *Chem. Phys. Lett.* **1994**, *218*, 133. (d) Rösch, N.; Görling, A.; Ellis, D. E.; Schmidbaur, H. *Angew. Chem., Int. Ed. Engl.* **1989**, *28*, 1357.

(9) (a) Schmidbaur, H. *Gold Bull.* **1990**, *23*, 11. (b) Schmidbaur, H. *Chem. Soc. Rev.* **1995**, *24*, 391. (c) Schmidbaur, H. *Interdiscip. Sci. Rev.* **1992**, *17*, 213. (d) Schmidbaur, H. *Gold Bull.* **2000**, *33*, 1. (e) *Gold: Progress in Chemistry, Biochemistry and Technology*; Schmidbaur, H., Ed.; J. Wiley and Sons: Chichester, U.K., 1999.

(10) Bondi, A. *J. Phys. Chem.* **1964**, *68*, 441.

(11) (a) Puddephatt, R. J. *Coord. Chem. Rev.* **2001**, *216−217*, 313. (b) Brandys, M.-C.; Puddephatt, R. J. *J. Am. Chem. Soc.* **2001**, *123*, 4839. (c) McArdle, C. P.; Jennings, M. C.; Vittal, J. J.; Puddephatt, R. J. *Chem. Eur. J.* **2001**, *7*, 3572. (d) McArdle, C. P.; Irwin, M. J.; Jennings, M. C.; Vittal, J. J.; Puddephatt, R. J. *Chem. Eur. J.* **2002**, *8*, 723. (e) Mohr, F. R.; Jennings, M. C.; Puddephatt, R. J. *Angew. Chem., Int. Ed.* **2004**, *43*, 969.

(12) (a) Hartgerink, J. D.; Clark, T. D.; Ghadiri, M. R. *Chem. Eur. J.* **1998**, *4*, 1367. (b) Ghadiri, M. R.; Kobayashi, K.; Granja, J. R.; Chadha, R. K.; McRee, D. E. *Angew. Chem., Int. Ed. Engl.* **1995**, *34*, 93.

(13) (a) Qin, Z.; Jennings, M. C.; Puddephatt, R. J. *Chem. Commun.* **2002**, 354. (b) Muthu, S.; Yip, J. H. K.; Vittal, J. J. *J. Chem. Soc., Dalton Trans.* **2002**, 4561. (c) Muthu, S.; Yip, J. H. K.; Vittal, J. J. *J. Chem. Soc., Dalton Trans.* **2001**, 3577. (d) Schauer, C. L.; Matwey, E.; Fowler, F. W.; Lauher, J. W. *Cryst. Eng.* **1998**, *1*, 213.

Experimental Section

General Information. All reactions were performed under a nitrogen atmosphere, and solvents for syntheses (analytical grade) were used without further purification. (***Caution:*** *Perchlorate salts are potentially explosive and should be handled with care and in small amounts*.) NMR data were obtained on a Bruker DPX 400 MHz NMR, using deuterated solvents with the usual standards. UV−vis spectra were recorded on a Perkin-Elmer Lambda 19 spectrophotometer and steady-state emission spectra on a SPEX Fluorolog-2 spectrophotometer. Solvents for photophysical studies were purified by literature methods, and solutions for photophysical experiments were degassed by at least four freeze−pump−thaw cycles. *N*,*N*′-Bis-4-methylpyridyl oxalamide was prepared by a literature method.[14]

Synthesis. [L(AuPPh$_3$)$_2$](ClO$_4$)$_2$, 1. The reaction of **L** (13.5 mg, 0.05 mmol) dissolved in CH_2Cl_2/MeOH (1:1, 25 mL) with $AuPPh_3(NO_3)$ [obtained from $AuCl(PPh_3)$ (49 mg, 0.1 mmol) and $AgNO_3$ (20.4 mg, 0.12 mmol) in CH_2Cl_2/MeOH (1:1, 25 mL)] at room temperature for 4 h gave a colorless solution. The solution was filtered, and the filtrate was concentrated to ca. 5 mL. Addition of excess $LiClO_4$ yielded a white solid. Recrystallization of the crude product by diffusion of diethyl ether into a dimethylformamide solution afforded colorless crystals with a 70% yield. ^{1}H NMR (400 MHz, DMSO-d_6, 25 °C): δ 4.53 [d, 2H, NCH_2], 7.66 [m, 17H, PPh_3 + (CH)$_2$C], 8.82 [d, 2H, −N(CH)$_2$], 9.58 [t, 1H, −NH]. ^{31}P NMR shows a singlet at δ = 30.07 ppm. FT-IR: ν_{NH} = 3237 cm^{-1}, $\nu_{C=O}$ = 1697 cm^{-1}, ν_{Cl-O} = 1081 cm^{-1}. ESI-MS: [M − (2 × ClO_4)], *m*/*e* = 594.2, 6%. Anal. Calcd (%) for $C_{50}H_{44}Au_2Cl_2N_4O_{10}P_2$: C, 43.28; H, 3.20; N, 4.04. Found (%): C, 42.93; H, 3.29; N, 4.21.

[dppm(Au$_2$)L]$_2$(ClO$_4$)$_4$, 2. The reaction of **L** (27 mg, 0.1 mmol) dissolved in CH_2Cl_2/MeOH (1:1, 25 mL) with dppm$(AuNO_3)_2$ [obtained from dppm$(AuCl)_2$ (85 mg, 0.1 mmol) and $AgNO_3$ (37.4 mg, 0.22 mmol) in CH_2Cl_2/MeOH (1:1, 50 mL)] at room temperature for 4 h gave a colorless solution. The solution was filtered, and the filtrate was concentrated to ca. 5 mL. Addition of excess $LiClO_4$ yielded a white solid. Recrystallization of the crude product by diffusion of diethyl ether into a dimethylformamide solution afforded colorless crystals with a 75% yield. ^{1}H NMR (400 MHz, DMSO-d_6, 25 °C): δ 4.59 [d, 2H, NCH_2], 4.72 [t, 1H, PCH_2], 7.44−7.88 [m, 10H, PPh_2],7.53 [d, 2H, (CH)$_2$C], 8.62 [d, 2H, −N(CH)$_2$], 9.85 [t, 1H, −NH]. ^{31}P NMR shows a singlet at δ = 29.28 ppm. FT-IR: ν_{NH} = 3311 cm^{-1}, $\nu_{C=O}$ = 1671 cm^{-1}, ν_{Cl-O} = 1088 cm^{-1}. ESI-MS: [M − (4 × ClO_4)], *m*/*e* = 524.7, 100%; [M − (2 × ClO_4)], *m*/*e* = 1148.8, 6%. Anal. Calcd (%) for $C_{78}H_{72}Au_4Cl_4N_8O_{20}P_4$: C, 37.55; H, 2.91; N, 4.49. Found (%): C, 37.87; H, 3.09; N, 4.11.

[dppp(Au$_2$)L]$_2$(ClO$_4$)$_4$, 3. This was synthesized by a method similar to the preparation of **2**. Recrystallization of the crude product by diffusion of diethyl ether into an ethanol/dimethylformamide solution afforded colorless crystals with a 65% yield. ^{1}H NMR (400 MHz, DMSO-d_6, 25 °C): δ 2.04 [s, 1H, −CH_2−], 3.09 [s, 2H, PCH_2], 4.56 [d, 2H, NCH_2], 7.58−7.90 [m, 12H, PPh_2 +(CH)$_2$C], 8.64 [d, 2H, −N(CH)$_2$], 9.61 [t, 1H, −NH]. ^{31}P NMR shows a singlet at δ = 26.72 ppm. FT-IR: ν_{NH} = 3334 cm^{-1}, $\nu_{C=O}$ = 1679 cm^{-1}, ν_{Cl-O} = 1092 cm^{-1}. ESI-MS: [M − (4 × ClO_4)], *m*/*e* = 538.2, 51%; [M − (2 × ClO_4)], *m*/*e* = 1221.6, 64%. Anal. Calcd (%) for $C_{82}H_{80}Au_4Cl_4N_8O_{20}P_4$: C, 38.61; H, 3.16; N, 4.39. Found (%): C, 38.87; H, 3.01; N, 4.51.

{[(dpppn)$_{3.5}$(Au$_7$)L$_{3.5}$](PF$_6$)$_7$}, 4. This was also synthesized by a method similar to the preparation of **2**, except using NH_4PF_6 instead of $LiClO_4$. Recrystallization of the crude product by diffusion of diethyl ether into a methanol/dimethylformamide solution afforded colorless crystals with a 65% yield. ^{1}H NMR (400 MHz, DMSO-d_6, 25 °C): δ 1.58 [m, 3H, −CH_2CH_2CH_2−], 2.74 [t, 2H, PCH_2], 4.49 [d, 2H, NCH_2], 7.55−7.92 [m, 12H, PPh_2 +(CH)$_2$C], 8.78 [d, 2H, −N(CH)$_2$], 9.60 [t, 1H, −NH]. ^{31}P NMR shows a singlet at δ = 29.22 ppm. FT-IR: ν_{NH} = 3365 cm^{-1}, $\nu_{C=O}$ = 1679 cm^{-1}. Anal. Calcd (%) for $C_{150.5}H_{154}Au_7F_{42}N_{14}O_7P_{14}$: C, 37.03; H, 3.18; N, 4.02. Found (%): C, 36.82; H, 3.57; N, 4.39.

X-ray Crystallography. Suitable crystals were mounted on glass capillaries. Data collection was carried out on a Bruker SMART CCD diffractometer with Mo radiation (0.71073 Å) at 273 K for **1** and 150 K for **2**·4Et$_2$O, **3**·2H$_2$O·4EtOH, and **4**·H$_2$O·2CH$_3$OH·5C$_3$H$_7$NO, respectively. A preliminary orientation matrix and unit cell parameters were determined from 3 runs of 15 frames each, each frame corresponding to 0.3° scan in 15 s, followed by spot integration and least-squares refinement. Data were measured using an ω scan of 0.3° per frame for 20 s until a complete hemisphere had been collected. Cell parameters were retrieved using SMART[15] software and refined with SAINT[16] on all observed reflections. Data reduction was performed with the SAINT software and corrected for Lorentz and polarization effects. Absorption corrections were applied with the program SADABS.[16] The structure was solved by direct methods with the SHELX93[17] program and refined by full-matrix least-squares methods on F^2 with SHEXLTL-PC V 5.03.[18] All non-hydrogen atomic positions were located in difference Fourier maps and refined anisotropically. The hydrogen atoms were placed in their geometrically generated positions. Detailed data collection and refinement of the four complexes are summarized in Table 1. Selected bond distances and angles are summarized in Table 2. Hydrogen bonds in the structures of complexes **1**, **2**·4Et$_2$O, and **3**·2H$_2$O·4EtOH are given in Table 3.

Results and Discussion

Complexes **1**, **2**, **3**, and **4** were prepared by treating $AuPPh_3(NO_3)$ or $PP(AuNO_3)_2$ (PP = dppm, dppp, dpppn) with **L** in CH_2Cl_2/MeOH, with yields of 65−75% (Schemes 1 and 2). Suitable single crystals with solvates (except **1** without any solvate) were grown by ether diffusion into a DMF solution for **1** and for **2**, an ethanol/DMF solution for **3**, and a methanol/DMF solution for **4**. All of the compounds are formed by self-assembly reactions, and the isolated products are colorless and luminescent both in solution and in the solid state. Whereas a related system had been previously reported by Puddephatt et al. on luminescent gold(I) macrocycles with diphosphines and 4,4′-bipyridyl ligands,[19] where the dppm, dppp, and dpppn all form rectangular structures in the solid state with diphosphines having a *syn* conformation, the dipyridyl−amide systems reported here with the amides incorporated into the bridging ligands feature interesting metal-containing cyclic peptides.

(14) Fraser, C. S. A.; Eisler, D. J.; Jennings, M. C.; Puddephatt, R. J. *Chem. Commun.* **2002**, 1224.

(15) *SMART V 4.043 Software for the CCD Detector System*; Siemens Analytical Instruments Division: Madison, WI, 1995.

(16) *SAINT V 4.035 Software for the CCD Detector System*; Siemens Analytical Instruments Division: Madison, WI, 1995.

(17) Sheldrick, G. M. *SHELXL-93, Program for the Refinement of Crystal Structures*; University of Gottingen: Gottingen, Germany, 1993.

(18) *SHELXTL 5.03 (PC-Version), Program Liberary for Structure Solution and Molecular Graphics*; Siemens Analytical Instruments Division: Madison, WI, 1995.

(19) Brandys, M.-C.; Jennings, M. C.; Puddephatt, R. J. *J. Chem. Soc., Dalton Trans.* **2000**, 4601.

Table 1. Crystallographic Data for **1**, **2**·4Et_2O, **3**·2H_2O·4EtOH, and **4**·H_2O·2CH_3OH·5C_3H_7NO

	1	**2**·4Et_2O	**3**·2H_2O·4EtOH	**4**·H_2O·2CH_3OH·5C_3H_7NO
empirical formula	$C_{50}H_{44}Au_2Cl_2N_4O_{10}P_2$	$C_{94}H_{112}Au_4Cl_4N_8O_{24}P_4$	$C_{90}H_{110}Au_4Cl_4N_8O_{26}P_4$	$C_{167.5}H_{199}Au_7F_{42}N_{19}O_{15}P_{14}$
fw	1387.69	2791.51	2773.45	5328.82
cryst syst	triclinic	triclinic	monoclinic	monoclinic
space group (No.)	$P\bar{1}$	$P\bar{1}$	$P2_1/c$	$C2/c$
a (Å)	9.661(2)	13.1777(2)	14.6031(3)	42.8041(11)
b (Å)	13.856(3)	14.5761(2)	26.1358(5)	30.9919(8)
c (Å)	22.7057(7)	15.4089(2)	14.9999(3)	31.2315(8)
α (°)	73.873(3)	88.3923(9)	90	90
β (°)	76.235(3)	83.1850(8)	119.0110(9)	106.499(1)
γ (°)	67.152(3)	67.5237(9)	90	90
V (Å^3)	1247.4(4)	2715.1(1)	5006.59(17)	39725.1(18)
Z	2	1	2	8
ρ_{calcd} (g cm^{-3})	1.847	1.704	1.838	1.778
F(000) (e)	674	1366	2712	20720
μ (Mo Kα) (mm^{-1})	6.107	5.613	6.090	5.363
T (K)	295(2)	150(1)	150(1)	150(1)
λ (Å)	0.71073	0.71073	0.71073	0.71073
reflns collected	14966	44752	25659	163254
indep reflns	5919 (R_{int} = 0.030)	12439 (R_{int} = 0.055)	7963 (R_{int} = 0.065)	34998 (R_{int} = 0.081)
obsd reflns ($F_o \geq 2\sigma(F_o)$)	5919	12439	7963	34998
refined params	337	563	594	2233
GOF on F^2	1.025	1.103	1.044	1.013
R,[a] R_w[b]($I \geq 2\sigma(I)$)	0.036, 0.076	0.060, 0.169	0.049, 0.126	0.082, 0.189
R,[a] R_w[b](all data)	0.047, 0.080	0.090, 0.188	0.071, 0.141	0.133, 0.224
ρ_{fin} (max/min) (e Å^{-3})	0.976/−0.400	2.718/−1.631	2.954/−2.748	5.626/−4.136

[a] $R = \sum||F_o| - |F_c||/\sum|F_o|$. [b] wR2 = $[\sum w(|F_o|^2 - |F_c^2|)^2/\sum w|F_o|^2]^{1/2}$.

Table 2. Selected Bond Distances (Å) and Angles (deg) for **1**, **2**, **3**, and **4**

compd				
1	Au(1)−N(1)	2.078(3)	Au(1)−P(1)	2.2359(11)
	N(1)−Au(1)−P(1)	174.68(11)		
2	Au(1)−N(1)	2.080(7)	Au(1)−P(1)	2.235(2)
	Au(2)−N(2)	2.088(6)	Au(2)−P(2)	2.239(2)
	Au(1)−Au(2)	3.1484(4)		
	N(1)−Au(1)−P(1)	171.3(2)	N(2)−Au(2)−P(2)	175.41(18)
3	Au(1)−N(1)	2.081(7)	Au(1)−P(1)	2.231(2)
	Au(2)−N(4)	2.074(7)	Au(2)−P(2)	2.237(2)
	N(1)−Au(1)−P(1)	175.66(17)	N(4)−Au(2)−P(2)	177.48(19)
4	Au(1)−N(1)	2.077(11)	Au(1)−P(1)	2.229(3)
	Au(2)−N(2)	2.068(11)	Au(2)−P(2)	2.235(4)
	Au(3)−N(5)	2.087(14)	Au(3)−P(3)	2.239(5)
	Au(4)−N(6)	2.063(16)	Au(4)−P(4)	2.229(4)
	Au(5)−N(9)	2.073(15)	Au(5)−P(5)	2.229(5)
	Au(6)−N(10)	2.096(15)	Au(6)−P(6)	2.231(4)
	Au(7)−N(13)	2.044(13)	Au(7)−P(7)	2.216(4)
	N(1)−Au(1)−P(1)	172.7(3)	N(2)−Au(2)−P(2)	177.4(4)
	N(5)−Au(3)−P(3)	178.2(4)	N(4)−Au(4)−P(4)	173.6(6)
	N(9)−Au(5)−P(5)	177.7(4)	N(10)−Au(6)−P(6)	179.6(6)
	N(13)−Au(7)−P(7)	177.4(5)		

Table 3. Hydrogen Bonds in the Structures of **1**, **2**, and **3**[a]

complex	D−H···A (Å)	D−H (Å)	H···A (Å)	D···A (Å)	D−H···A (deg)
1	N(2)−H(2A)···O(5)[(a)]	0.86	2.352	3.020(7)	134.8
2	N(3)−H(3A)···O(2A)[(b)]	0.88	2.094	2.855(10)	144.3
	N(4)−H(4A)···O(6A)[(c)]	0.88	2.346	3.163(13)	154.5
3	N(3)−H(3A)···O(1A)[(d)]	0.88	2.029	2.810(10)	147.5
	N(2)−H(2A)···O(6A)[(e)]	0.88	2.062	2.848(12)	148.4

[a] Symmetry positions of atoms A: (a) 1 + x, 1 + y, z; (b) 1 − x, −y, −z; (c) 1 − x, 1 − y, −z; (d) 1 − x, 1 − y, 1 − z; (e) −x, 1 − y, −z.

Description of Crystal Structure. Perspective views of complexes **1**, **2**, **3**, and **4** are shown in Figures 1 − 4, respectively. The gold(I) centers are all two-coordinate, each coordinating to pyridyl and phosphine groups in an almost linear geometry with P−Au−N angles ranging from 171.3(2) ° to 179.6(6)°. The Au−P distances [2.216(4)−2.239(2) Å] and Au−N distances [2.044(13)−2.096(15) Å] fall in the normal range and are also comparable to those values reported by Puddephatt et al.[19] Any close intermolecular gold(I)···gold(I) contact seems to be prevented by the bulky phosphine ligands for the four gold(I) compounds studied here.

Scheme 1

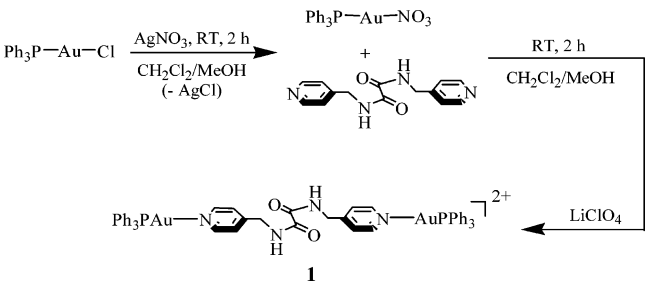

Scheme 2

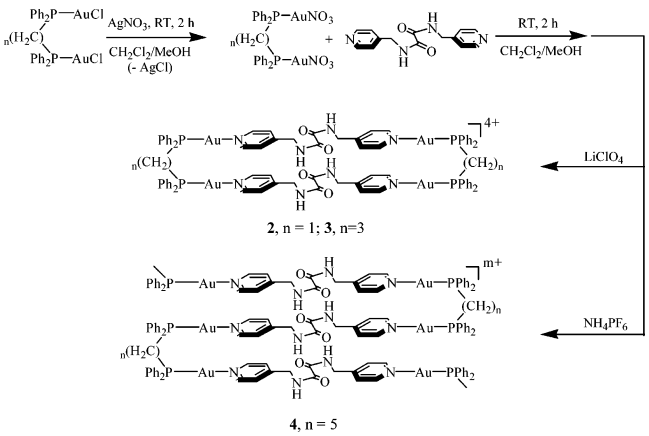

As shown in Figure 1a, complex **1** is a dinuclear gold(I) compound with **L** acting as a bridging ligand. Each gold(I) center also coordinates to one triphenylphosphine. Interestingly, there are weak intermolecular $\pi\cdots\pi$ stacking interac-

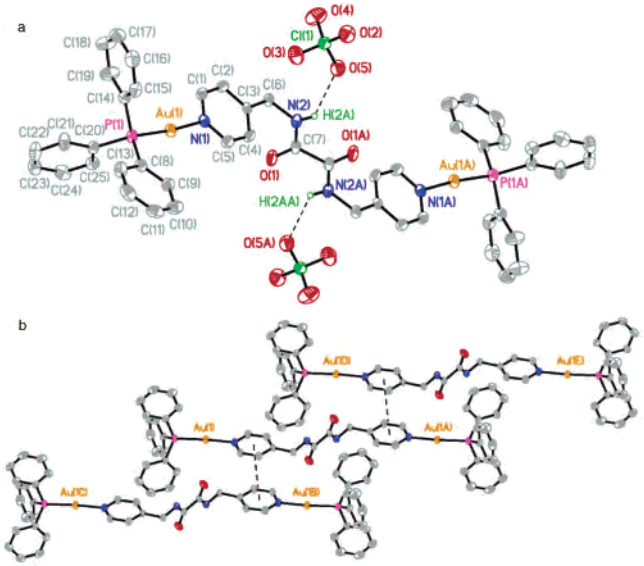

Figure 1. (a) Molecular structure of $\mathbf{1}\cdot(ClO_4)_2$ with ORTEP diagram showing 50% probability ellipsoids. (b) The molecular packing showing $\pi\cdots\pi$ interactions leading to the formation of one-dimensional chains.

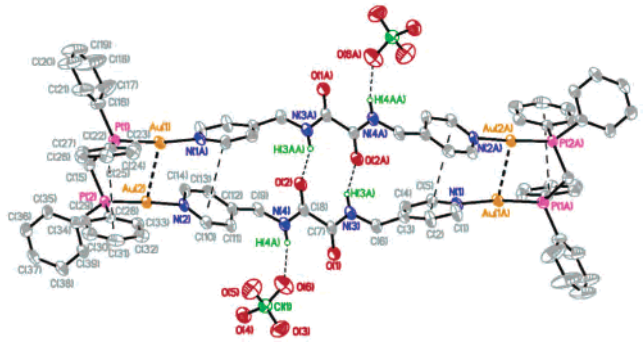

Figure 2. Molecular structureof **2** with ORTEP diagram showing 50% probability ellipsoids.

tions (centroid to centroid distance: 3.954 Å; angle between centroid → centroid vector and any normal to pyridyl rings: ca. 27.6°),[20] between two parallel pyridyl rings leading to the formation of a one-dimensional chain structure as Figure 1b. However, the centroid to centroid distance of 3.954 Å seems somewhat long, possibly due to packing forces (dispersion interactions). Hydrogen-bonding interactions between the amide moiety of **L** and the $O-ClO_3^-$ anion [N(2)−H(2A)···O(5), N(2)···O(5) 3.020(7) Å] are observed in the solid state. The rodlike structure of **1** has a P···P distance of 20.85 Å.

The combination of $PP(AuNO_3)_2$ (PP = dppm or dppp) and 1 equiv of **L** is a rational design of molecular rectangles (or macrocycles), where the dppm and dppp are both anticipated to adopt *syn* conformations in this assembly process. Indeed, molecular rectangles of **2** and **3** are successfully synthesized, isolated, and characterized, and their crystal structures have been determined by X-ray diffraction studies at 150 K. The perspective views of complexes **2** and **3** are shown in Figures 2 and 3a, respectively. Complex cation **2** adopts a rectangular structure, featuring a 38-membered ring with four gold(I) ions at the

(20) Janiak, C. *J. Chem. Soc., Dalton Trans.* **2000**, 3885.

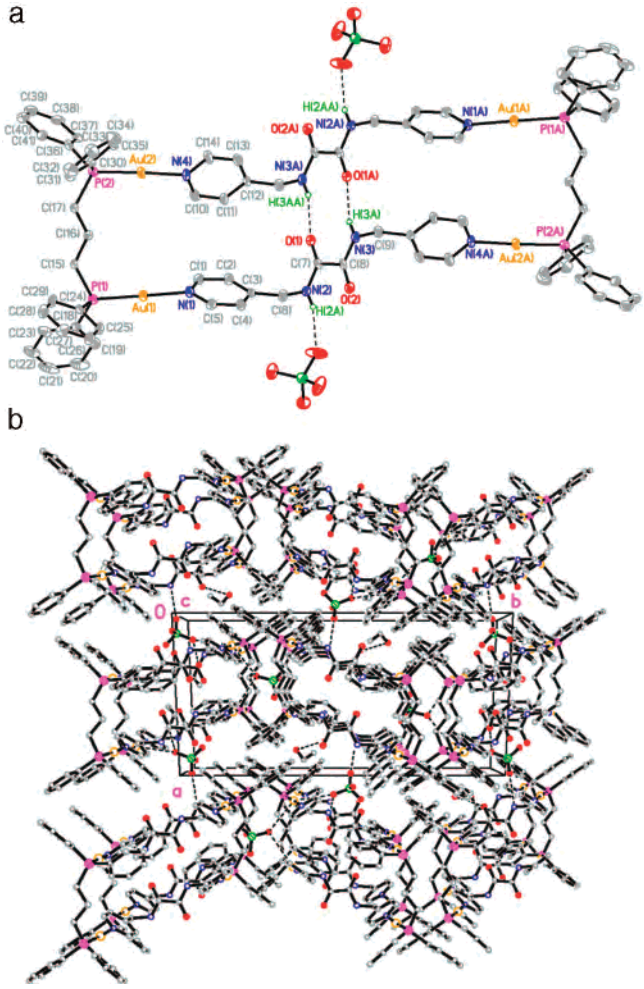

Figure 3. (a) Molecular structureof **3** with ORTEP diagram showing 50% probability ellipsoids. (b) The molecular packing showing one-dimensional channel structures in the solid state.

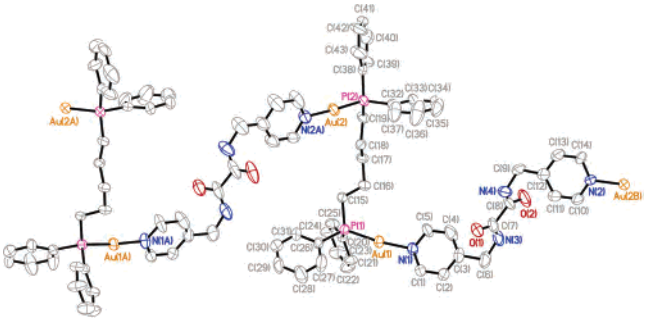

Figure 4. Molecular structureof cation **4** shows one-dimensional chain structure.

corners as well as two **L** and two dppm as edges. The transannular Au(1)···Au(2) distance is 3.1484(4) Å, which is less than the sum of the van der Waals radii of gold(I) ions (3.32 Å), indicating the presence of aurophilic interactions. Although the distance is slightly longer than the values of 3.1061(8) and 3.0841(8) Å in the 4,4′-bipyridyl analogue,[19] this could be reconciled by the oxygen atom of the triflate anion simultaneously binding to two gold(I) centers of the $dppmAu_2$ moiety. The amide−amide hydrogen bonding is present inside the rectangle, where two inward N−H groups are each hydrogen-bonded to the inward C═O groups.

Additionally, two outward N−H groups are each hydrogen-bonded to O−ClO_3^- [N(3)−H(3A)···O(2A), N(3)···O(2A) 2.855(10) Å; N(4)−H(4A)···O(6A), N(4)···O(6A) 3.163(13) Å]. The area inside the rectangular cavity is roughly 3.05 × 20.81 Å^2 based on the distances between the P atoms. There are also weak intramolecular $\pi\cdots\pi$ stacking interactions between pyridyl or phenyl rings (centroid to centroid distances: 4.025 Å for pyridyl pairs and 3.753 Å for phenyl pairs; dihedral angles between two pyridyl or phenyl rings: 32.5° for pyridyl pairs and 17.4° for phenyl pairs; angles between centroid → centroid vector and any normal to pyridyl rings: ca. 20.7° for pyridyl pairs and ca. 13.6° for phenyl pairs).[20] Since there is deviation from parallel for the dihedral angles (32.5° and 17.4°), C−H···π interactions can also be used to rationalize these stacking interactions.[20] Unfortunately, complex **2** cannot form one-dimensional rectangular channels in the solid state as the Re(I)-based rectangles reported by Lu et al.[6] However, this is a rare example which simultaneously exhibits a variety of weak interactions within a single molecule.

Cation **3** also adopts a rectangular structure, featuring a 42-membered ring with four gold(I) ions at the corners, as well as two **L** and two dppp ligands as edges. The transannular Au(1)···Au(2) distance is 5.510 Å, indicating the absence of any significant aurophilic interaction. The distance is again slightly longer than the value of 5.279(1) Å in the 4,4′-bipyridyl analogue,[19] and this should be also ascribed to binding interactions between the oxygen atom of a triflate anion and two gold(I) centers of the dpppAu_2 moiety. The area inside the rectangular cavity is roughly 5.55 × 20.66 Å^2 based on the distances between the P atoms. Amide−amide hydrogen bonding occurs inside the rectangle, where two inward N−H groups are each hydrogen-bonded to the inward C═O groups, and additionally two outward N−H groups are each hydrogen-bonded to O−ClO_3^- [N(3)−H(3A)···O(1A), N(3)···O(1A) 2.810(10) Å; N(2)−H(2A)···O(6A), N(2)···O(6A) 2.848(12) Å]. The centroid to centroid distance of 4.171 Å for pyridyl rings inside the cavity seems too long for any possibility of intramolecular $\pi\cdots\pi$ interactions. Nevertheless, there exist weak intermolecular $\pi\cdots\pi$ stacking interactions between the pyridyl rings (centroid to centroid distance: 3.715 Å; dihedral angle between two pyridyl rings: 1.1°; angles between centroid → centroid vector and any normal to pyridyl rings: ca. 20.6°).[20] Unlike that of **2**, the packing of cation **3** shows one-dimensional rectangular channels in the solid state as shown in Figure 3b, and this is most likely ascribed to the presence of intermolecular $\pi\cdots\pi$ interactions.

It is somewhat surprising that, whereas complexes **2** and **3** form molecular rectangles, cation **4** has been isolated and structurally characterized as a one-dimensional coordination polymer as shown in Figure 4 (only one independent polymer chain shown). In comparison, its 4,4′-bipyridyl analogue has been shown to have a rectangular structure.[19] Cation **4** has a complex structural framework containing four independent polymer chains in an asymmetric unit, with alternating dpppnAu_2 and **L**Au_2 units leading to the formation of zigzag chains. Among them, three polymer chains have no symmetry element for dpppn, but the last one has a 2-fold axis passing through the center of dpppn. Thus, the repeating units of [(dpppn)(Au_2)**L**](PF_6)$_2$ for each of the three independent polymer chains, and of [(dpppn)$_{0.5}$(Au)**L**$_{0.5}$](PF_6) for the last one, constitute an asymmetric unit. The four polymer chains do not pack parallel to each other, and the conformation of independent polymer chains shows little difference. However, the supramolecular assembly of similar ligand systems resulting in different structural frameworks is not uncommon.[18a,21] The difference in the structural motifs may be due to the more flexible backbone for **L** compared with the 4,4′-bipyridyl moiety and/or packing forces, and thus the dpppn is forced to adopt an *anti* conformation in complex **4**.

The PF_6^- salts of dppm and dppp have also been isolated and characterized[22] to compare with those of the ClO_4^- salts. Although the crystal structures of the related PF_6^- salts cannot be determined at this moment, the spectroscopic data did suggest that the structures are independent of the anions. One possible reason the structures of the dppm and dppp complexes with rectangular structures are not dependent on anions (ClO_4^- and PF_6^-) used is that the amide−amide hydrogen bonding is present inside the cavity, where two inward N−H groups are each hydrogen-bonded to the inward C═O groups. This double hydrogen bonding may be expected to stabilize these rectangular structures. Additionally, two outward N−H groups are each hydrogen-bonded to ClO_4^- outside the cavity, and thus the anions can show little effect on the structural conformation.

The supramolecular assembly of diphosphines and *N*,*N*′-bis-4-methylpyridyl oxalamides studied here is largely consistent with the bipyridyl systems reported by Puddephatt et al.[19] A comparison shows that the dppm and dppp complexes form molecular rectangles in both systems, but it is surprising that a different structural motif was found for the two complexes of dpppn. Whereas the bipyridine and dpppn complexes also gave rise to a rectangular structure, the more flexible *N*,*N*′-bis-4-methylpyridyl oxalamide and dpppn complex is a one-dimensional coordination polymer with a zigzag structure. Actually, the molecular mechanics

(21) (a) Qin, Z.; Jennings, M. C.; Puddephatt, R. J. *Inorg. Chem.* **2003**, *42*, 1956. (b) Tabellion, F. M.; Seidel, S. R.; Arif, A. M.; Stang, P. J. *Angew. Chem., Int. Ed.* **2001**, *40*, 1529. (c) Tabellion, F. M.; Seidel, S. R.; Arif, A. M.; Stang, P. J. *J. Am. Chem. Soc.* **2001**, *123*, 7740. (d) Fang, J.; Sun, W.-Y.; Okamura, T.-a.; Zheng, Y.-Q.; Sui, B.; Tang, W.-X.; Ueyama, N. *Cryst. Growth Des.* **2004**, *4*, 579. (e) Horikoshi, R.; Mochida, T.; Kurihara, M.; Mikuriya, M. *Cryst. Growth Des.* **2005**, *5*, 243. (f) Zhang, G.; Yang, G.; Chen, Q.; Ma, J. S. *Cryst. Growth Des.* **2005**, *5*, 661. (g) Burchell, T. J.; Eisler, D. J.; Jennings, M. C.; Puddephatt, R. J. *Chem. Commun.* **2003**, 2228.

(22) Data for [dppm(Au_2)**L**]$_2$(PF_6)$_4$ follow. ^{1}H NMR (400 MHz, DMSO-d_6, 25 °C): δ 4.58 [d, 2H, NCH_2], 4.73 [t, 1H, PCH_2], 7.43−7.88 [m, 10H, PPh_2], 7.52 [d, 2H, (CH)$_2$C], 8.62 [d, 2H, −N(CH)$_2$], 9.84 [t, 1H, −NH]. ^{31}P NMR shows a singlet at δ = 29.26 ppm. ESI-MS: [M − (4 × PF_6)], *m*/*e* = 524.7, 85%; [M − (2 × PF_6)], *m*/*e* = 1148.8, 16%. Anal. Calcd (%) for $C_{78}H_{72}Au_4Cl_4N_8O_{20}P_4$: C, 34.99; H, 2.71; N, 4.19. Found (%): C, 34.82; H, 2.52; N, 3.87. Data for [dppp(Au_2)-**L**]$_2$(PF_6)$_4$ follow. ^{1}H NMR (400 MHz, DMSO-d_6, 25 °C): δ 2.03 [s, 1H, −CH_2−], 3.08 [s, 2H, PCH_2], 4.56 [d, 2H, NCH_2], 7.57−7.90 [m, 12H, PPh_2 +(CH)$_2$C], 8.63 [d, 2H, −N(CH)$_2$], 9.62 [t, 1H, −NH]. ^{31}P NMR shows a singlet at δ = 26.71 ppm. ESI-MS: [M − (4 × PF_6)], *m*/*e* = 538.2, 65%; [M − (2 × PF_6)], *m*/*e* = 1221.6, 16%. Anal. Calcd (%) for $C_{82}H_{80}Au_4Cl_4N_8O_{20}P_4$: C, 36.03; H, 2.95; N, 4.10. Found (%): C, 36.28; H, 2.80; N, 3.95.

Table 4. Spectroscopic and Photophysical Data of **1**, **2**, **3**, and **4**

compd	λ_{abs} (nm)/CH_3CN ϵ ($dm^3\,mol^{-1}\,cm^{-1}$)	$\lambda_{em}{}^a$ (nm) solid state (RT)	$\lambda_{em}{}^a$ (nm) solution/CH_3CN
1	232/20700 266/2700	424, 449, 478, 515	462
2	263/15700	465	424
3	253/14800	442	423
4	233/20600 268/2400	427	450

[a] Photoexcitation for both solid state and solution is at 300−325 nm.

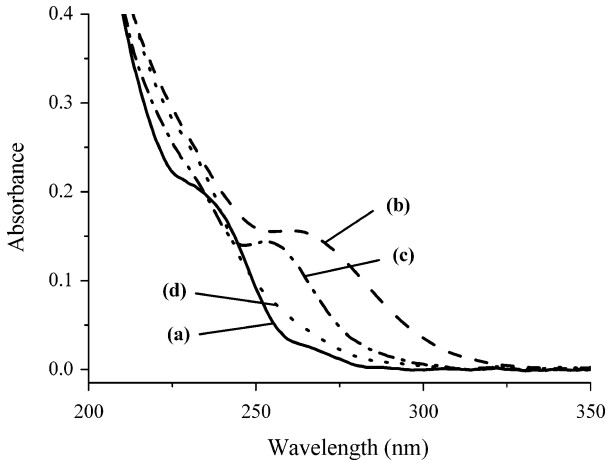

Figure 5. The absorption spectra of **1** (a), **2** (b), **3** (c), and **4** (d) measured in CH_3CN at a concentration of 10^{-5} M.

calculations[19] predicted that, with the bipyridyl ligand, the dppm and dppp gold(I) complexes would gain stabilization energies of up to −18 and −10 kcal mol^{-1}, respectively, in the macrocyclic form. However, the corresponding dpppn complex was found to be stabilized by −1 kcal mol^{-1} in the macrocyclic form. This energy may be readily compensated or competitive by any weak interaction present in the solid state, and thus the structural change from a macrocycle to a coordination polymer is not unexpected.[18a,21] The *N*,*N*′-bis-4-methylpyridyl oxalamide studied herein has been demonstrated to increase supramolecular complexity by additional hydrogen bonding compared with the bipyridyl analogue. Thus, **2** provides an interesting example in which to investigate various intramolecular interactions, i.e., hydrogen-bonding, $\pi\cdots\pi$, and aurophilic interactions, cooperatively present in the same molecule. In addition, the dipyridyl amide system with the amides incorporated into the bridging ligands as well as the one-dimensional rectangular channels in the solid state for **3** make this family of metal-containing cyclic peptides interesting candidates for crystal engineering and molecular-recognition studies.

Spectroscopic and Photophysical Properties. UV−Vis Absorption Spectra. Spectroscopic and photophysical data are listed in Table 4, and the absorption spectra of complexes **1**, **2**, **3**, and **4** measured in CH_3CN are shown in Figure 5. In general, complexes **1**−**4** only show high-energy absorptions at 232−268 nm with a tailing to 300−325 nm. On the basis of the similarity to those of **L** and the respective phosphines, these high-energy absorptions are most likely ascribed to intraligand transitions in origin, perturbed through coordination to gold(I) ions. A detailed assignment of such bands, however, is prevented by band overlapping (**L**, 257 nm; PPh_3, 262 nm; dppm, 265 nm). A similar assignment regarding the high-energy absorptions of a gold(I)−amido system with 2,2′-bibenzimidazolate as a bridging ligand has previously been made by Che et al.[23]

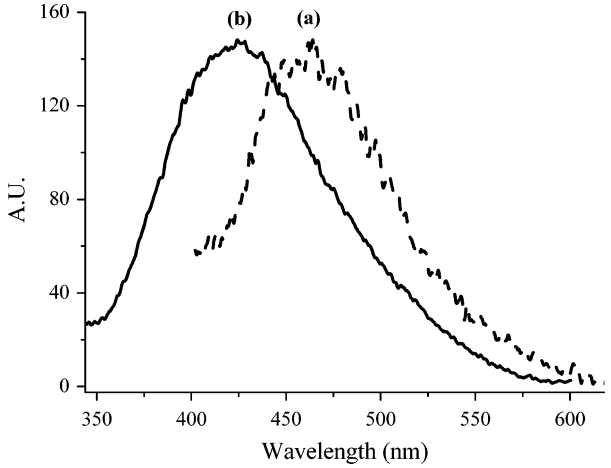

Figure 6. The emission spectra of **2** measured in the solid state (a) and in CH_3CN (b) at a concentration of 10^{-5} M upon photoexcitation at 300−325 nm.

On the basis of amide−amide hydrogen bonding occurring inside the rectangle, it was expected that complexes **2** and **3** would retain their rectangular structures in solution, but complex **2** shows a red shift (∼10 nm) compared with complex **3**. Since **2** is the only complex which shows intramolecular gold(I)···gold(I) interactions in this study, the red shift is possibly attributed in part to the aurophilic interaction. With reference to the literature studies,[24] the red shift in transition energy due to gold(I)···gold(I) interactions is not uncommon in d^{10}−d^{10} systems, where the 290 nm band is assigned to the 5d($d\sigma^*$) → 6p($p\sigma$) transition in $[Au_2(dppm)_2]^{2+}$ with a gold(I)···gold(I) distance of 2.962(1) Å. In fact, the absorption band of **2** has a tailing to 325 nm, and this coincides with the above rationale.

Emission Spectra. As representative example, the emission spectra of complex **2** measured in the solid state and in a degassed CH_3CN solution are shown in Figure 6. The emission data of all the compounds measured in the solid state and in solution are compiled in Table 4. Upon photoexcitation at 300−325 nm, complex **2** shows luminescence at 465 and 424 nm in the solid state and in solution, respectively, at room temperature. With reference to previous studies[19,23] and compared with the emissions of gold(I) phosphine halides [$AuClPPh_3$ and $dppm(AuCl)_2$ luminesce at 430−460 nm], the 465 and 424 nm emissions are tentatively assigned to an intraligand transition of phosphines. The red shift from 424 nm in CH_3CN to 465 nm in the solid state for **2** is also observed for **3** (423 nm in CH_3CN and 442 nm in the solid state). To explain this trend, the structural data of **2** and **3** are compared. The distances of 3.290−3.360

(23) Tzeng, B.-C.; Li, D.; Peng, S.-M.; Che, C.-M. *J. Chem. Soc., Dalton Trans.* **1993**, 2365.
(24) (a) Che, C.-M.; Kwong, H.-L.; Yam, V. W.-W.; Cho, K.-C. *J. Chem. Soc., Chem. Commun.* **1989**, 885. (b) King, C.; Wang, J.-C.; Khan, M. N. I.; Fackler, J. P., Jr. *Inorg. Chem.* **1989**, *28*, 2145.

Å (**2**) and 3.500 Å (**3**) are the shortest distances between the C (N) and C (N) atoms of the pyridyl or phenyl rings, whereas the values of 4.025/3.753 Å (**2**) and 3.715 Å (**3**) are the centroid to centoid distances between the pyridyl or phenyl rings. Although the centroid to centoid distances of 3.753 Å (**2**) and 3.715 Å (**3**) are only indicative of the presence of weak $\pi\cdots\pi$ interactions,[20] the spectroscopic properties modified by these weak interactions are still possible.[25] Thus, the red shift ascribed to the intramolecular $\pi\cdots\pi$ interactions for **2** and the intermolecular $\pi\cdots\pi$ interactions for **3** seems reasonable on the basis of the solid-state structures. That **2** shows a greater red shift relative to that of **3** is consistent with shorter $\pi\cdots\pi$ distances indicative of stronger $\pi\cdots\pi$ interactions for **2**.

In contrast to the above trend, the red shift is observed from 427 nm in the solid state to 450 nm in degassed CH_3CN for **4**, and this is a common effect due to the environment.[26] Compound **1** shows an emission band at 462 nm in solution and broad and structured emission bands at 424, 449, 478, and 515 nm in the solid state. Indeed, these emissions are quite comparable to those of the bipyridyl analogues, mostly ascribed to intraligand transitions of phosphines in origin.[19] However, it should be noted that the possibility of the emissions in this spectral region being from the Au → phosphines charge-transfer transition could not be excluded.[27]

Conclusion

We report herein the supramolecular assembly and spectroscopic and luminescent properties of gold(I) compounds with diphosphines (i.e., dppm, dppp, and dpppn) and *N*,*N*′-bis-4-methylpyridyl oxalamide. The compounds are isolated at moderate yields of 65−75% and structurally characterized by crystallographic studies. The dppm and dppp complexes form the rectangular structures with four gold(I) ions at the corners, as well as two **L** and two dppm or dppp ligands as edges, featuring 38- and 42-membered rings, respectively. The dppm-based rectangle is a rare example of a complex exhibiting a variety of weak interactions simultaneously within a single molecule. Remarkably, the packing of the dppp-based rectangle shows interesting one-dimensional rectangular channels in the solid state, and this is most likely a contribution from the intermolecular $\pi\cdots\pi$ interactions. The spectroscopic data suggest that the rectangular structures are independent of the anions (ClO_4^- and PF_6^-) used. One possible reason is that the amide−amide hydrogen bonding is present inside the cavity, where two inward N−H groups are each hydrogen-bonded to the inward C═O groups. This double hydrogen bonding may be expected to stabilize these rectangular structures. Additionally, two outward N−H groups are each hydrogen-bonded to ClO_4^- outside the cavity, and thus the anions can show little effect on the structural conformation.

It is somewhat surprising that, unlike the complexes of dppm and dppp, which form molecular rectangles, the dpppn complex has been structurally characterized as a one-dimensional coordination polymer. The absorptions and emissions of the compounds are mostly due to intraligand transitions in origin, but the aurophilicity or $\pi\cdots\pi$ interactions could also play a partial role. In this context, a red shift in emission energies from the solution to solid state for dppm- and dppp-based rectangles has been observed.

The dipyridyl amide ligand has been chosen and used as a bridging ligand instead of the bipyridine studied by Puddephatt et al,[19] because the amide−amide hydrogen bonding and flexibility are anticipated to increase the supramolecular complexity and interactions. The dipyridyl amide system with the amides incorporated into the bridging ligands as well as the one-dimensional rectangular channels in the solid state for the dppp-based rectangle make this interesting family of metal-containing cyclic peptides promising candidates for crystal engineering studies, such as the use of the complex (rectangle) as a ligand after deprotonation of the amides, and for molecular-recognition studies, such as the shape-directed sensing of VOCs or heavy-metal ion binding.

Acknowledgment. We thank the National Science Council and National Chung Cheng University of the Republic of China for financial support.

Supporting Information Available: Crystallographic data in cif format. This material is available free of charge via the Internet at http://pubs.acs.org.

IC051297A

(25) Cheung, T.-C.; Cheung, K.-K.; Peng, S.-M.; Che, C.-M. *J. Chem. Soc., Dalton Trans.* **1996**, 1645.
(26) (a) Wrighton, M.; Morse, D. L. *J. Am. Chem. Soc.* **1974**, *96*, 998. (b) Connick, W. B.; Miskowski, V. M.; Houlding, V. H.; Gray, H. B. *Inorg. Chem.* **2000**, *39*, 2585.
(27) Larson, L. J.; McCauley, E. B.; Weissbart, B.; Tinti, D. S. *J. Phys. Chem.* **1995**, *99*, 7218.